Inertial Measurement Unit for Radiation-Free Navigated Screw Placement in Slipped Capital Femoral Epiphysis Surgery

Bamshad Azizi Koutenaei[1,2], Ozgur Guler[1], Emmanuel Wilson[1], Matthew Oetgen[1], Patrick Grimm[1], Nassir Navab[2,3], and Kevin Cleary[1]

[1] Children's National Medical Center, Washington D.C, United States
{bazizi,oguler,ewilson,moetgen,pgrimm,kcleary}@cnmc.org
[2] Chair for Computer Aided Medical Procedures (CAMP), TUM, Munich, Germany
[3] Computer Aided Medical Procedures (CAMP), Johns Hopkins University, USA
nassir@cs.tum.edu

Abstract. Slipped Capital Femoral Epiphysis (SCFE) is a common pathologic hip condition in adolescents. In the standard treatment, a surgeon relies on multiple intra-operative fluoroscopic X-ray images to plan the screw placement and to guide a drill along the intended trajectory. More complex cases could require more images, and thereby, higher radiation dose to both patient and surgeon. We introduce a novel technique using an Inertial Measurement Unit (IMU) for recovering and visualizing the orthopedic tool trajectory in two orthogonal X-ray images in real-time. The proposed technique improves screw placement accuracy and reduces the number of required fluoroscopic X-ray images without changing the current workflow. We present results from a phantom study using 20 bones to perform drilling and screw placement tasks. While dramatically reducing the number of required fluoroscopic images from 20 to 4, the results also show improvement in accuracy compared to the manual SCFE approach.

Keywords: Slipped Capital Femoral Epiphysis (SCFE), Computer-assisted Orthopedic Surgery, Computer-aided Intervention, Inertial Measurement Unit.

1 Introduction

Computer-assisted surgery (CAS) has been used in various clinical procedures. Surgical planning methods for image guidance fall within two broad categories: volumetric image-based navigation (primarily, CT and MRI) and intraoperative fluoroscopic navigation [1]. Both methods could be used in passive and active CAS systems [2]. CAS systems have found increased use particularly in orthopedic surgery, where surgeon interaction is largely with rigid anatomy that is immobilized with relative efficacy. In many orthopedic procedures, the surgeon relies heavily on intra-operative fluoroscopic images; from planning implant trajectory, to guiding intra-operative positioning, and finally, to confirming implant position at completion. Antirotator proximal femoral nailing and intramedullary nailing of femur fracture are examples of

N. Navab et al. (Eds.): MICCAI 2015, Part I, LNCS 9349, pp. 355–362, 2015.
DOI: 10.1007/978-3-319-24553-9_44

orthopedic procedures that broadly follow this approach with regards to image acquisition. The pre-operative fluoroscopic images are crucial in planning the procedure, and post-operative images are needed to validate procedural accuracy. The number of additional images acquired during the procedure to orient and reposition a tool depend on surgeon skill and experience, and leads to increased radiation dose and procedure times. For instance, the average number of fluoroscopy images used for distal locking was 48.27 that causes significant radiation exposure [3]. Therefore many augmented reality systems proposed to reduce radiation exposure during the surgery for instance: half-mirror display devices [4], single laser-beam pointers [5], video see-through binocular systems [6] visualization based on IMU [7], systems that directly project images onto the patient's body [8], and other radiation-free drill guidance for orthopedic surgery [9][10][11][12].

Therefore we introduce a system in this paper that could reduce radiation dose, while improving implant accuracy with applicability in many orthopedic procedures. As a case study we chose slipped capital femoral epiphysis (SCFE) surgery.

SCFE is a common hip disorder that causes displacement of the proximal femoral epiphysis. Traditional surgical treatment requires placing screws from the proximal femoral metaphysis into the femoral head for stabilization of the proximal femoral epiphysis (Fig. 1). In the conventional approach to SCFE, the surgeon uses intra-operative fluoroscopic imaging as visualization aid to guide the screw placement and confirm the drill trajectory.

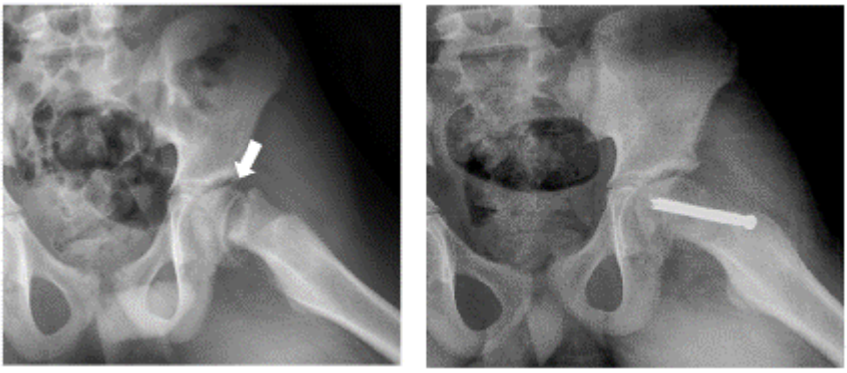

Fig. 1. (Left) radiograph of a SCFE case (arrow). (Right) fixation of the SCFE

In regards to the placement of implants to treat SCFE, a navigation system based on inertial measurement unit (IMU) could help reduce both radiation dose and procedure time. Therefore we implemented a system that superimposes IMU information onto two orthogonal fluoroscopic images.

2 Methodology

A conventional SCFE procedure uses intra-operative fluoroscopic images for visualization to accurately place the screw. This causes significant radiation exposure for

both surgeon and patient. A typical work-flow involves the surgeon extrapolating a tool entry point based on target site and optimal tool orientation using fluoroscopic images. Once an optimal tool trajectory is evaluated, additional X-ray images are acquired to confirm that the tool is being inserted along this planned path. On average, about 20 x-ray images are acquired to deduce the best orientation and guide the tool during the procedure. The question we asked is: "What new information of clinical utility are these additional x-ray images providing?" Once a surgeon has mapped out the procedural workflow using pre-operative planning images, these additional images serve no clinical utility beyond confirming tool orientation. Our approach was to use a relatively inexpensive hardware device to augment this information in lieu of x-ray image. We were able to register and super-impose the real-time tool trajectory on two pre-operative orthogonal x-ray images. This results in improving screw placement and greatly decreased radiation exposure.

We chose an Inertial Measurement Unit (IMU) because of its compact size, low cost, and accurate orientation representation. The IMU used for this system is an X-IMU (x-io Technologies, Bristol, UK). The device consists of a 3-axis gyroscope, 3-axis accelerometer, and a 3-axis magnetometer. It sends combined data from the various sensors encapsulated in each data packet. Data transfer is done over Bluetooth LowEnergy (BLE) wireless protocol to our application running on a laptop at a rate of 512 packets per second. The laptop application uses a sensor fusion algorithm [13] to calculate the current orientation. We designed a 3D-printed fixture which mounts to the drill base and houses the IMU device. This provides a fixed, known relation between the drill bit and IMU. We used an Epiphan DVI2USB3.0 frame-grabber (Epiphany Systems Inc., Palo Alto, CA) to frame-grab the x-ray images from the Siemens Zeego system. To facilitate a more ergonomic surgeon experience, we streamed the laptop visualization to a Samsung tablet placed next to the surgeon.

In this paper, we introduce two different methods to assist the surgeon. In method (A) we use one image, one pivot point placed on the bone to identify an entry point, and a calibrated IMU placed within the image plane. In method (B) we use two orthogonal x-ray images and four points (1 pivot point and three fiducials for coordinate registration). No additional calibration of the IMU is required in the latter approach.

Pre-operative Set-up: In method (A), we used a 3D-printed calibration fixture to align the IMU to the patient table coordinate, shown in Fig 2a. During the procedure, we used a second 3D-printed fixture to affix the IMU to the drill, shown in Figure 2b. The IMU calibration fixture orients the IMU XY-plane with the A-P fluoroscopic image plane, and IMU YZ-plane with the lateral fluoroscopic plane. The patient table position and Zeego robot coordinates are inherently calibrated. Therefore, by orienting the IMU coordinate frame with respect to the patient table, we have a calibration between fluoroscopic image plane and the IMU coordinates. For method (B), the registration between IMU and fluoroscopic image coordinates is done based on selection of four corresponding points in each pair of orthogonal x-ray images. The four points are comprised of the drill tip and three 8mm diameter metal sphere fiducials, shown in Fig 2c.

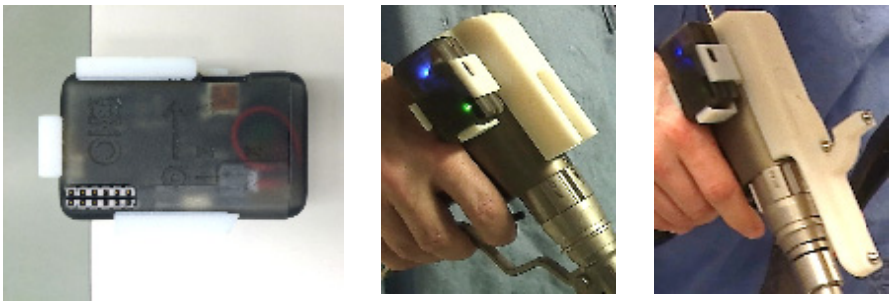

(a) **(b)** **(c)**

Fig. 2. (a) Calibration fixture (b) Drill fixture (c) Fiducial spheres for coordinate registration

Intra-Operative Planning: Here we explain the two methods employed to register the drill coordinates to image space in real-time.

Method (A): The surgeon identifies an entry point by drilling a small divot at the bone surface. Two orthogonal x-rays images are acquired (in A-P and Lateral orientations). As mentioned before, in this method navigation can be based off one image alone. However, image augmentation and navigation was done using both the A-P and Lateral images, as this approach is clinically most relevant. After loading those images in our application, we define the drill tip as a pivot point. We use seed based region growing segmentation to choose the best possible pivot point in a semi-automatic manner. Subsequently, the IMU is placed within the calibration fixture and placed at the edge of the patient table. The calibration fixture was designed such that it orients the IMU coordinates in a known configuration with respect to image coordinates. Based on our setting, the IMU X-Y plane maps to the A-P image plane and the IMU Y-Z frame maps to the lateral image (Error < 0.6 mm). Afterward, our method projects the updated orientation to two orthogonal images. These two projections are calculated by the following chain of transformations, and shown in Figure 3.

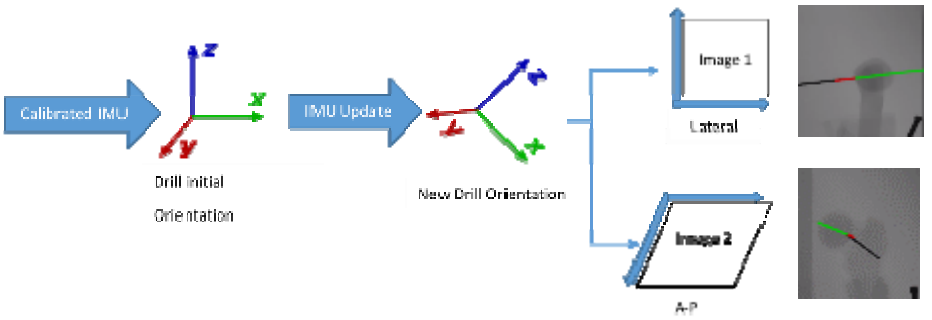

Fig. 3. Flow chart of method (A) transformation chain

T is a 4x4 transformation matrix, P is a projection matrix, and Tr is a translation matrix. (IMU = device, WRD = World defined by IMU, IMG = C-arm)

$$^{Pivot}Tr_{XY} * {}^{XY}P_{IMG} * {}^{IMG}T_{WRD} * {}^{WRD}T_{IMU} \quad (1)$$

$$^{Pivot}Tr_{YZ} * {}^{YZ}P_{IMG} * {}^{IMG}T_{WRD} * {}^{WRD}T_{IMU} \quad (2)$$

Method (B): The surgeon defines the entry point and drills into the bone surface to create an identifying divot point. The drill is fixed besides the table using a passive arm such that the drill tip is within the divot. Two orthogonal x-ray images (AP and Lateral) that visualize the drill tip and the three fiducials are acquired. After loading the images in our application, the three fiducials and drill tip are identified in commensurate order in both AP and Lateral images. We used a seed based region growing segmentation to choose the best possible pivot point and also center of the spheres in a semi-automatic manner. The application calculates the 3D position of those fiducial points by combining selected point positions in the two images (we obtain x and y coordinates from AP, and z coordinate from the Lateral image). With this we calculate the transformation between world coordinates to image coordinates. Since the drill bit is aligned precisely to the X-axis of the IMU, our application projects the x-axis of the IMU in the AP and Lateral images (Error < 0.8 mm). These two projections are calculated by the following chain of transformation, shown in Figure 4.

T is a 4x4 transformation matrix, P is a projection matrix, and Tr is a translation matrix. (IMU = device, WRD = World defined by IMU, IMG = C-arm)

$$^{Pivot}Tr_{XY} * {}^{XY}P_{IMG} * {}^{IMG}T_{Drill} * {}^{Drill}T_{IMUi} * {}^{IMUi}T_{WRD} * {}^{WRD}T_{IMUup} \quad (3)$$

$$^{Pivot}Tr_{YZ} * {}^{YZ}P_{IMG} * {}^{IMG}T_{Drill} * {}^{Drill}T_{IMUi} * {}^{IMUi}T_{WRD} * {}^{WRD}T_{IMUup} \quad (4)$$

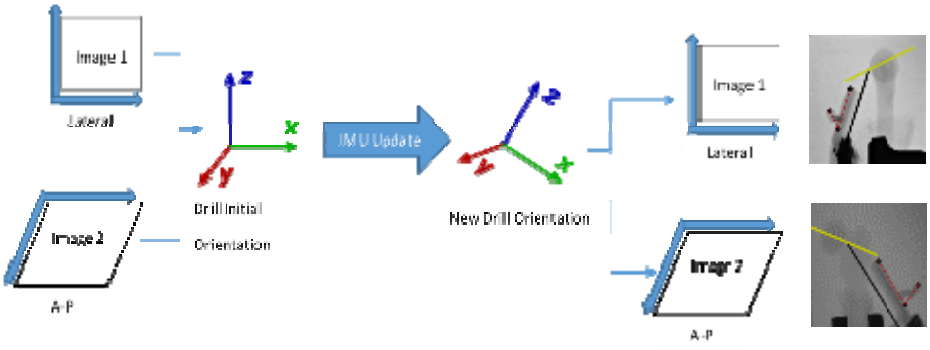

Fig. 4. Flow chart of method (B) transformation chain

Post-Operative Verification: Once the surgeon plans a path, the application collects and logs IMU orientation data until the surgeon has drilled to the target location. Once at the target location, a pair of confirmatory AP and Lateral images are acquired to correctly identify actual drill position. Post-operative validation is achieved by comparing the planned drill trajectory to actual, as shown in Fig 5.

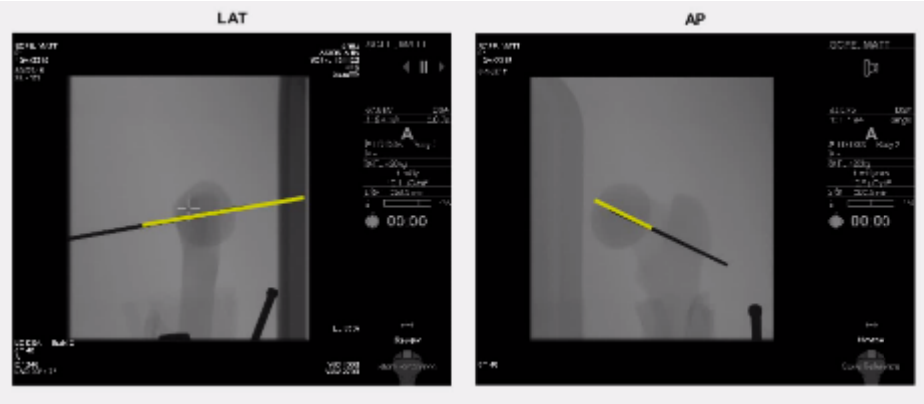

Fig. 5. Post x-ray evaluation in Lateral and A-P (yellow line is the trajectory before drilling)

3 Results

We started the study by assessing the accuracy of the x-IMU device using a Polaris optical tracker (Northern Digital Inc., Waterloo, Canada). In addition, the internal report of X-IMU shows the IMU device and algorithm we used is highly accurate[1]. The first proof-of-concept test in the lab used two orthogonal images with a standard smartphone camera to assess the efficacy of this approach. These tests confirmed the validity of our concept. Following lab tests, we completed a study in the operating room, including image acquisition from the Siemens Zeego C-arm system.

Left femur bone models with slipped capital epiphysis deformity (Model # 1161, Sawbones Worldwide, Vashon Island, WA) were used to perform the drilling and screw placement tasks, shown in Figure 6. 10 manual procedures were performed by the experienced surgeon, which served as baseline assessment of the procedural accuracy and completion time. Subsequently, 30 assisted trials were performed by the experienced orthopedic surgeon, and another 10 assisted trials performed by an orthopedic resident with no experience in SCFE surgery. For each trial, the total procedure time and number of fluoroscopic images acquired were logged, and the final placement accuracy computed from confirmatory orthogonal images acquired at the end of each trial. Average procedure time for the manual trials was 2:46 (mm:ss). Average procedure time was 1:51 (mm:ss) for the assisted trials for the experienced surgeon and 4:31 (mm:ss) for the non-experienced surgeon. The longer procedure time for the assisted trials for the non-experienced surgeon can be in part attributed to considerations given to learning curve and set-up time. The accuracy results show clear improvement with the assisted trials. Pending a study on a larger number of data samples, this shows sufficient accuracy in comparison to the conventional [14] and robotic-assisted approach [15]. The results are shown in Table 1.

[1] http://www.x-io.co.uk/res/doc/madgwick_internal_report.pdf

Table 1. 10 manual and 40 navigated trials conducted by experienced and non-experienced surgeon. Total error is measured for target points based on distance of desired and drilled points (Statistical Significance: $p < 0.05$, Registration Error: Err < 0.8 mm).

	Skill in SCFE	Total time	# of images	Total error
10 Manual	Experienced	2:46	20.4	7.6 mm
30 Assisted	Experienced	1:51	4	3.59 mm
10 Assisted	Non-Experienced	4:31	4	6.35 mm

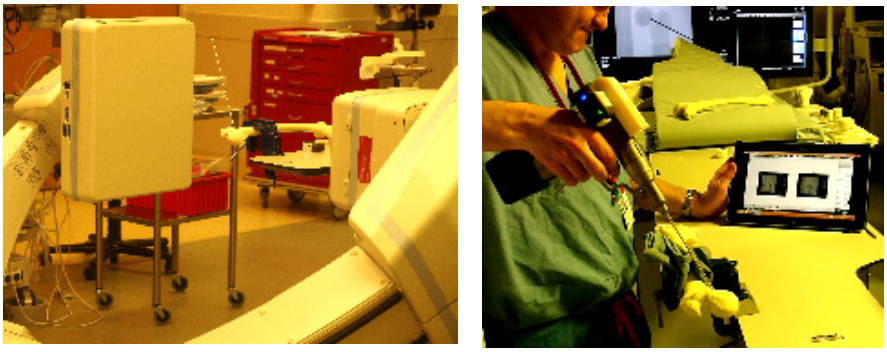

(a) **(b)**

Fig. 6. Phantom study in interventional suite. (a) Setup for lateral exposure (b) Surgeon using the visualization for planning optimal tool path

4 Conclusion and Future Work

Slipped capital femoral epiphysis is a relatively common orthopedic procedure in children where the accurate placement of the fixation screw often requires 20 x-ray images or a CT dataset in a conventional approach. This paper introduces a simple, cost-effective system to assist surgeons in intra-operative path planning in a real-time manner based on an IMU device. With this device setup, and reliance on only two orthogonal x-ray images, we were able to streamline the SCFE procedure. In addition, these techniques could be extended to many other orthopedic procedures that follow a similar clinical workflow. This preliminary study shows promising results, both in overall radiation exposure reduction and improved accuracy to the conventional approach in a phantom study. In future, the system could be complemented by using a head mounted display and more sophisticated navigation and visualization tools. Our long term goal is to pursue a clinical trial to determine if this approach could lead to a more accessible SCFE workflow and improved clinical outcome for patients.

References

1. Sugano, N.: Computer-assisted orthopedic surgery. Journal of Orthopaedic Science 8(3), 442–448 (2003)
2. Musahl, V., Plakseychuk, A., Fu, F.H.: Current opinion on computer-aided surgical navigation and robotics: role in the treatment of sports-related injuries. Sports Med. 32(13), 809–818 (2002)
3. Rohilla, R., Singh, R., Magu, N., Devgan, A., Siwach, R., Sangwan, S.: Simultaneous use of cannulated reamer and schanz screw for closed intramedullary femoral nailing. ISRN Surg. (2011) (published online)
4. Liao, H., Ishihara, H., Tran, H.H., Masamune, K., Sakuma, I., Dohi, T.: Fusion of Laser Guidance and 3-D Autostereoscopic Image Overlay for Precision-Guided Surgery. In: Dohi, T., Sakuma, I., Liao, H. (eds.) MIAR 2008. LNCS, vol. 5128, pp. 367–376. Springer, Heidelberg (2008)
5. Marmurek, J., Wedlake, C., Pardasani, U., Eagleson, R., Peters, T.: Image-Guided Laser Projection for Port Placement in Minimally Invasive Surgery. Stud. Health Technol. Inform. 119, 367–372 (2006)
6. Fuchs, H., State, A., Pisano, E.D., Garrett, W.F., Hirota, G., Livingston, M., Whitton, M.C., Pizer, S.: Towards Performing Ultrasound-Guided Needle Biopsies from within a Head-Mounted Display. In: Höhne, K.H., Kikinis, R. (eds.) VBC 1996. LNCS, vol. 1131, pp. 591–600. Springer, Heidelberg (1996)
7. Walti, J., Jost, G.F., Cattin, P.C.: A New Cost-Effective Approach to Pedicular Screw Placement. In: Linte, C.A. (ed.) AE-CAI 2014. LNCS, vol. 8678, pp. 90–97. Springer, Heidelberg (2014)
8. Volonte, F., Pugin, F., Bucher, P., Sugimoto, M., Ratib, O., Morel, P.: Augmented Reality and Image Overlary Navigation with OsiriX in Laparoscopic and Robotic Surgery: Not Only a Matter of Fashion. J. Hepatobiliary Pancreat Sci. 18, 506–509 (2011)
9. Diotte, B., Fallavollita, P., Wang, L., Weidert, S., Thaller, P.-H., Euler, E., Navab, N.: Radiation-free drill guidance in interlocking of intramedullary nails. In: Ayache, N., Delingette, H., Golland, P., Mori, K. (eds.) MICCAI 2012, Part I. LNCS, vol. 7510, pp. 18–25. Springer, Heidelberg (2012)
10. Hoffmann, M., et al.: Next generation distal locking for intramedullary nails using an electromagnetic X-ray-radiation-free real-time navigation system. Journal of Trauma and Acute Care Surgery 73, Jg., Nr. 1, 243–248 (2012)
11. Stathopoulos, I., et al.: Radiation-free distal locking of intramedullary nails: Evaluation of a new electromagnetic computer-assisted guidance system. Injury, 44. Jg., Nr. 6, 872–875 (2013)
12. Arlettaz, Y., et al.: Distal locking of femoral nails: evaluation of a new radiation independent targeting system. Journal of Orthopaedic Trauma 26. Jg., Nr. 11, S. 633–637 (2012)
13. Madgwick, S.O.H., Harrison, A.J.L., Vaidyanathan, R.: Estimation of IMU and MARG orientation using a gradient descent algorithm. In: 2011 IEEE International Conference Rehabilitation Robotics (ICORR), pp. 1–7 (2011), doi:10.1109/ICORR.2011.5975346
14. Pring, E.M., Adamczyk, M., Hosalkar, H.S., Bastrom, T.P., Wallace, C.D., Newton, P.O.: In situ screw fixation of slipped capital femoral epiphysis with a novel approach: a double-cohort controlled study. Journal of Children's Orthopaedics 4(3), 239–244 (2010)
15. Azizi Koutenaei, B., Guler, O., Wilson, E., et al.: Improved Screw Placement for Slipped Capital Femoral Epiphysis (SCFE) using Robotically-Assisted Drill Guidance. In: International Conference on Medical Image Computing and Computer-Assisted Intervention, vol. 17(01), pp. 488–495 (2014)